Available online at www.sciencedirect.com
ScienceDirect
Metabolic Engineering 9 (2007) 228–239
METABOLIC ENGINEERING
www.elsevier.com/locate/ymben

Magnetic nanofactories: Localized synthesis and delivery of quorum-sensing signaling molecule autoinducer-2 to bacterial cell surfaces

Rohan Fernandes[a,b], Chen-Yu Tsao[b,c], Yoshifumi Hashimoto[b], Liang Wang[b,d], Thomas K. Wood[e], Gregory F. Payne[b], William E. Bentley[a,b,c,*]

[a]Fischell Department of Bioengineering, University of Maryland, College Park, MD 20742, USA
[b]Center for Biosystems Research, University of Maryland Biotechnology Institute, College Park, MD 20742, USA
[c]Department of Chemical and Biomolecular Engineering, University of Maryland, College Park, MD 20742, USA
[d]Department of Cell Biology and Molecular Genetics, University of Maryland, College Park, MD 20742, USA
[e]Department of Chemical Engineering, Texas A&M University, College Station, TX 77843, USA

Received 9 June 2006; received in revised form 3 October 2006; accepted 29 November 2006
Available online 15 December 2006

Abstract

Magnetic 'nanofactories', for localized manufacture and signal-guided delivery of small molecules to targeted cell surfaces, are demonstrated. They recruit nearby raw materials for synthesis, employ magnetic mobility for capture and localization of target cells, and deliver molecules to cells triggering their native phenotypic response, but with user-specified control. Our nanofactories, which synthesize and deliver the ''universal'' bacterial quorum-sensing signal molecule, autoinducer AI-2, to the surface of Escherichia coli, are assembled by first co-precipitating nanoparticles of iron salts and the biopolymer chitosan. E. coli AI-2 synthases, Pfs and LuxS, constructed with enzymatically activatable ''pro-tags'', are then covalently tethered onto the chitosan. These enzymes synthesize AI-2 from metabolite S-adenosylhomocysteine. Chitosan serves as a molecular scaffold and provides cell capture ability; magnetite provides stimuli responsiveness. These magnetic nanofactories are shown to modulate the natural progression of quorum-sensing activity. New prospects for small molecule delivery, based on localized synthesis, are envisioned.

Keywords: Magnetic particles; Quorum sensing; Localized synthesis and delivery; Immobilized enzymes; AI-2

1. Introduction

Localized delivery of a molecule-of-interest to a target cell surface is important in cell signaling (Shiner et al., 2005; Truckses et al., 2006; Wang et al., 2006; Yang et al., 2006). When delivered locally, a signaling molecule can produce a higher signal intensity that elicits an enhanced cellular response. For example, the localized delivery of growth factors has been shown to stimulate growth in targeted cells or tissue (Geer et al., 2005; Shansky et al., 2006; Wei et al., 2006). Various strategies have been employed to locally deliver signal molecules to target cells viz. using viral vectors (Taylor et al., 2006), degradable polymeric scaffolds (Holland et al., 2006), liposomes (Lee et al., 2005) and nanoparticles (Chung et al., 2006). All the above methods deliver signal molecules in their final form to their respective target cells. In this proof-of-concept paper, we are working with a novel and potentially programmable approach for the localized synthesis and delivery of a signaling molecule to a target cell surface using a magnetic 'nanofactory', which consists of enzymes with activatable 'pro-tags' conjugated to functionalized magnetic nanoparticles. Our technique differs from the above techniques in that it synthesizes the signal molecule from a precursor molecule at the surface of the target cell and locally delivers it (via the nanofactory). The rationale

*Corresponding author. University of Maryland, 5115 Plant Science Building #036, College Park, MD 20742, USA. Fax: +1 301 314 9075.
E-mail address: bentley@eng.umd.edu (W.E. Bentley).

1096-7176/$ - see front matter © 2006 Elsevier Inc. All rights reserved.
doi:10.1016/j.ymben.2006.11.004

behind employing such a mode of localized synthesis and delivery is that we can control the amounts of signal molecule delivered to the target cell thus potentially enabling an ex vivo fine-tuning of cellular response.

A nanofactory is a nano-sized factory that combines three attributes: an ability to 'manufacture' the signaling molecule (synthesis ability), an ability to bind to the cell surface (cell capture ability) thus localizing the synthesized signaling molecule to the cell surface and an ability to be directed and recovered in response to an external stimulus (stimuli responsiveness). We introduce 'nanofactories' by demonstrating their assembly via biologically benign techniques and their use by locally synthesizing and delivering the quorum-sensing (QS) signaling molecule autoinducer-2 (AI-2) at the surface of Escherichia coli cells. The appropriate AI-2-specific cell response confirms altered phenotypic behavior and a functioning 'programmable' nanofactory.

AI-2 is an inter- and intra-species signaling molecule that plays a role in QS (Fuqua et al., 1994), a process that mediates inter- and intra-species bacterial communication resulting in coordinated multicellular behavior. Diverse cell processes such as bioluminescence, biofilm formation, virulence, antibiotic production and competence (Gonzalez Barrios et al., 2006; Henke and Bassler, 2004; Vendeville et al., 2005; Waters and Bassler, 2005; Winzer et al., 2002; Xavier and Bassler, 2005) are in part, QS regulated. In E. coli, AI-2 is synthesized from S-adenosylhomocysteine (SAH) via a two-step enzymatic reaction involving the enzymes S-adenosylhomocysteine nucleosidase (Pfs) and S-ribosylhomocysteinase (LuxS) (Wang et al., 2005). To confer AI-2 synthesis ability to the nanofactories, the enzymes Pfs and LuxS are attached to functionalized magnetic nanoparticles using activatable "pro-tags" at their C-termini (Fig. 1).

In the first step, the magnetic carrier is synthesized by the dropwise addition of a mixture of ferric and ferrous salts ($[Fe^{3+}]/[Fe^{2+}] = 2$) and the biopolymer chitosan to a vigorously stirred base (NH_4OH) under an inert atmosphere. The resultant nano-sized co-precipitates contain both chitosan and magnetite (Fe_3O_4) called 'chitosan-mag' (Honda et al., 1998, 1999). Magnetite confers magnetic-responsiveness (stimuli responsiveness) to the nanofactory while chitosan serves a dual-role: it enables the nanofactory to attach to the target cell surface (cell capture ability) and it also provides amine-groups for attaching the enzymes Pfs and LuxS to the nanofactory. This dual-role of chitosan is related to its unique pH-dependent solubility. The amine-groups of chitosan have a pK_a of about 6.3 (Fernandes et al., 2003; Wu et al., 2002). At a pH below the pK_a, most amine-groups are protonated and chitosan is positively charged and water soluble; at pH above the pK_a, most amine-groups are deprotonated and chitosan is neutral and insoluble in water.

Pfs with a pentatyrosine pro-tag at its C-terminus [$(His)_6$-Pfs-$(Tyr)_5$] is covalently assembled onto the available surface chitosan in chitosan-mag by activation using the enzyme tyrosinase. Upon the addition of tyrosinase, the tyrosine residues in the pro-tag are activated and form o-quinones that can then react with the amine-groups of chitosan (Chen et al., 2001, 2002, 2003). Similarly, LuxS with the C-terminus pro-tag [$(His)_6$-LuxS-$(Tyr)_5$] is assembled onto chitosan-mag. The motivation for using pro-tags is that they are located at the C-termini of both Pfs and LuxS and extend away from their respective active sites. The addition of tyrosinase selectively activates the tyrosine residues of the tag and facilitates attachment of the enzymes via the tag to chitosan with intact enzymatic activity.

The nanofactories containing Pfs and those containing LuxS are then combined to obtain a suspension of magnetic nanofactories with AI-2 synthesis ability. These are added to a suspension containing the target cells (E. coli) where they bind to the cell surface via the available surface chitosan (Honda et al., 1998, 1999) (chitosan molecules without attached enzymes). The nanofactories

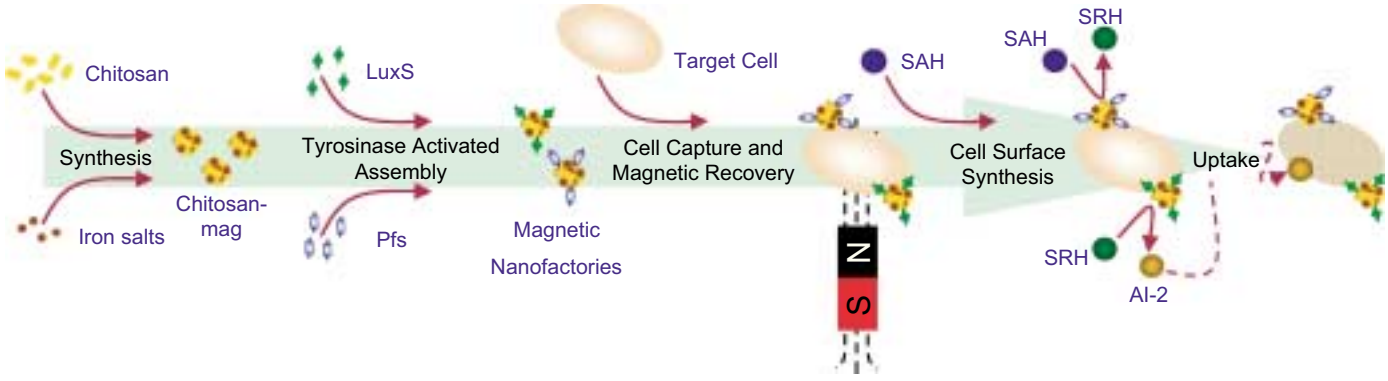

Fig. 1. Overview of assembly and use of nanofactories to locally synthesize and deliver QS signaling molecule, AI-2, to a target cell. Synthesis of the magnetic carrier, chitosan-mag, by co-precipitation of iron salts and chitosan; attachment of pro-tagged Pfs and LuxS to chitosan-mag by 'activation' using tyrosinase to assemble magnetic nanofactories; capture of target cells by the magnetic nanofactories; recovery of captured cells using an external magnet; cell surface synthesis and delivery of AI-2 by enzymes Pfs and LuxS; uptake of AI-2 and production of cellular response (AI-2-dependent reporter).

with the attached cells are recovered using an external magnetic field, resuspended in fresh medium or buffer and in vitro AI-2 is synthesized by the nanofactories, by addition of SAH, at the surface of the target cells. The in vitro synthesized AI-2 is delivered at the cell surface and taken up by the Lsr transporter producing an AI-2-specific transcriptional response, which is measured by β-galactosidase reporter activity. The interception of cell–cell communication and subsequent interruption of QS behavior is a topic of intense interest because downregulating specific cell functions (e.g., cell attachment, virulence) that lead to pathology, but are not essential for a pathogen's viability, may lower the rate of emergence of resistant strains. We believe nanofactories offer many advantages relative to the localized delivery of small molecules, in that the molecule could eventually be synthesized and delivered at a site, at a prescribed concentration and time.

2. Materials and methods

2.1. Chemicals

Chitosan (average molecular weight 50,000 g/mol), iron (II) chloride tetrahydrate ($FeCl_2 \cdot 4H_2O$), iron (III) chloride hexahydrate ($FeCl_3 \cdot 6H_2O$), isopropyl β-D-thiogalactopyranoside (IPTG), phosphate-buffered saline (PBS, 9.6 g/L), tyrosinase (from mushroom), S-(5′-deoxyadenosin-5′)-L-homocysteine (SAH), chloroform, sodium dodecyl sulfate salt (SDS, >98.5%), o-nitrophenyl-β-D-galactopyranoside (ONPG), 2-mercaptoethanol, imidazole, zinc acetate dehydrate, and glycerol were all purchased from Sigma Aldrich. Glacial acetic acid (CH_3COOH), ampicillin sodium salt, kanamycin, Tris, sodium carbonate (Na_2CO_3), dibasic sodium phosphate ($Na_2HPO_4 \cdot 7H_2O$), monobasic sodium phosphate ($NaH_2PO_4 \cdot H_2O$), potassium chloride (KCl), magnesium sulfate ($MgSO_4 \cdot 7H_2O$), sodium chloride were all purchased from Fisher Scientific. Ammonium hydroxide (NH_4OH) was purchased from J. T. Baker. 5-(and 6)-carboxyfluorescein succinimidyl ester (NHS-fluorescein) and ((4′-aminoacetamido) methyl) fluorescein (aminofluorescein) were purchased from Molecular Probes.

2.2. Synthesis of chitosan-mag and mag particles

A solution of chitosan (2.02% w/w, pH 5.5) was prepared as described elsewhere (Wu et al., 2002). A total of 9.9 mL (0.2 g) chitosan solution, 0.795 g of $FeCl_2 \cdot 4H_2O$ and 2.162 g of $FeCl_2 \cdot 4H_2O$ were dissolved in 40 mL double distilled water. This reaction mixture, which contains 0.5% chitosan, 0.2 M $[Fe^{3+}]$, 0.1 M $[Fe^{2+}]$ (i.e. $[Fe^{3+}]/[Fe^{2+}] = 2$), was purged with N_2 gas and added dropwise to vigorously stirred 2 M NH_4OH (pH 11.8), also previously purged with N_2). A positive N_2 pressure was maintained in the reaction chamber and care was taken to ensure that no bubbles were formed during the vigorous stirring (1500–2000 rpm). The resultant black precipitate that contains chitosan-mag particles was washed with copious amounts of double distilled water to remove the excess base and the pH of the suspension was brought to 7. For long-term storage, a 10 mg/mL suspension of chitosan-mag was prepared in 0.5% dilute acetic acid and stored at 4 °C for future use. For synthesis of mag, conditions identical to those for the synthesis of chitosan-mag were used. However, no chitosan solution was used in the synthesis of mag.

2.3. Bacterial strains and growth media

The bacterial strains used in this study are listed in Table 1. The Luria–Bertani broth contained 5 g/L of yeast extract (Sigma), 10 g/L of Bacto tryptone (Difco) and 10 g/L NaCl (J. T. Baker). The components of the Autoinducer Bioassay medium (AB) are described elsewhere (Bassler et al., 1994).

2.4. Plasmid construction

To express and purify Pfs with tyrosine tag (His-Pfs-Tyr) and LuxS with tyrosine tag (His-LuxS-Tyr), the plasmids pTrcHis-Pfs-Tyr and pTrcHis-LuxS-Tyr were constructed by PCR amplification of pfs (699 bp) and luxS (516 bp) from genomic DNA of E. coli strain W3110 (http://ecoli.aist-nara.ac.jp/) using the oligonucleotide primers listed in Table 1. PCR reactions were carried out by using PCR Master Mix (Promega) and followed by gel purification with QIAquick gel extraction kit (Qiagen). PCR products were digested with HindIII and XhoI, and the products were extracted by gel purification and then inserted into pTrcHisC (Invitrogen). To verify the integrity of all constructs, DNA sequencing was performed at the DNA core facility of the Center for Biosystems Research (University of Maryland Biotechnology Institute). To obtain purified His-Pfs-Tyr and His-LuxS-Tyr, pTrcHis-Pfs-Tyr and pTrcHis-LuxS-Tyr plasmids were transformed into DH5α (defective luxS) and NC13 (pfs knockout), respectively. In this way, there is no contaminating Pfs in LuxS preparations and vice versa.

2.5. Purification of $(His)_6$-Pfs-$(Tyr)_5$ and $(His)_6$-LuxS-$(Tyr)_5$

E. coli DH5α pTrcHis-Pfs-Tyr [for Pfs: $(His)_6$-Pfs-$(Tyr)_5$] and E. coli NC13 pTrcHis-LuxS-Tyr [for LuxS: $(His)_6$-LuxS-$(Tyr)_5$] were separately cultured at 37 °C and 250 rpm in LB medium supplemented with ampicillin at 50 μg/mL. When the optical densities (OD_{600}) of the cell cultures were between 0.4 and 0.6, IPTG was added to induce enzyme production (for Pfs culture: final concentration used was 1 mM IPTG, for LuxS culture: final concentration used was 1 mM IPTG and 0.1 mM zinc acetate). After 6 h, cells were collected by centrifugation at 6000g for 20 min at 4 °C. The cells were stored at −20 °C or directly resuspended in PBS + 10 mM imidazole. The resuspended cells were lysed by sonication using Sonic Dismembrator 550

Table 1
Bacterial strains, plasmids and oligonucleotide primers used in this study

Strain or plasmid	Relevant genotype and property	Reference
Escherichia coli strains		
W3110	Wild type	Laboratory stock
BL21	F′ ompT hsdS_B ($r_B^- m_B^-$) gal dcm	(Wu et al., 2000)
ZK126	Wild-type strain derivative, W3110 ΔlacU160-tna2	(Connell et al., 1987)
LW7	ZK126 ΔluxS::Kan	(Wang et al., 2005)
DH5α	recA1 supE44 endA1 hsdR17 gyrA96 relA1 thiΔ (lac-proAB) F′ [traD36 proAB+$lacI^q$ lacZΔM15]	Invitrogen
NC13	RK4353 Δpfs (8-226)::Kan	(Cadieux et al., 2002)
Vibrio harveyi strains		
BB170	BB120 luxN::Tn5 (sensor 1^-, sensor 2^+)	(Bassler et al., 1993)
Plasmids		
pGFP	pTrcHisB derivative, gfp^+, Amp^r	(Wu et al., 2000)
pTrcHis-LuxS-Tyr	pTrcHisC derivative, W3110 $luxS^+$, Amp^r	This study
pTrcHis-Pfs-Tyr	pTrcHisC derivative, W3110 pfs^+, Amp^r	This study
pFZY1	galK′-lacZYA transcriptional fusion vector, Amp^r	(Koop et al., 1987)
pLW11	pFZY1 derivative, containing lsrACDBFG promoter region, Amp^r	(Wang et al., 2005)

Oligonucleotide primers

Name	Sequence	Relevant property
PfsF	5′-CCGCTCGAGATATGAAAATCG GCATCATTG-3′	Upstream primer for cloning pfs from W3110 contains XhoI
5TyrPfsR	CCCAAGCTTTTAATAATAATAATAATAGCCATGTGCAAGTTTCTGCA	Downstream primer for cloning pfs from W3110 encodes 5-Tyr-tag and HindIII
LuxSF	CCGCTCGAGATATGCCGTTGTTAGATAGCT	Upstream primer for cloning luxS from W3110 contains XhoI
5TyrLuxSR	CCCAAGCTTCTAATAATAATAATAATAGATGTGCAGTTCCTGCAACT	Downstream primer for cloning luxS from W3110 encodes 5-Tyr-tag and HindIII

(Fisher Scientific). After sonication, the soluble cell extract was collected by centrifugation at 14,000g for 15 min at 4 °C. The soluble extract was filtered using a 0.22 μm polyether sulfone, low protein-binding filter (Millipore). The filtered extract was then loaded on a pre-equilibrated immobilized metal–ion affinity chromatography (IMAC) column (HiTrap Chelating HP, Amersham Biosciences). The sample was washed with varying amounts of phosphate buffer, sodium chloride and imidazole (Wash 1: 20 mM PO_4^{3-}, 250 mM NaCl and 10 mM imidazole; Wash 2: 20 mM PO_4^{3-}, 250 mM NaCl and 50 mM imidazole). The sample was then eluted with 20 mM PO_4^{3-}, 250 mM NaCl and 350 mM imidazole and dialyzed overnight into PBS at 4 °C. For long-term storage, glycerol was added to the enzyme solution (final glycerol concentration 30%) and the samples were stored at −80 °C until use.

2.6. Reaction with NHS-fluorescein and amino-fluorescein

Chitosan-mag and mag in dilute CH_3COOH (0.5 mg/mL, pH 6) were separately reacted with either NHS-fluorescein or amino-fluorescein in double-distilled water (5 μg/mL). The reaction mixture was maintained at pH 6 by PBS. The reaction was allowed to proceed at room temperature for 30 min. After reaction, the particles were recovered using a magnetic stand (Promega MagneSphere® stand Z5342). The particles were collected within 3 min. After collection, the particles were washed with copious amounts of double-distilled water and resuspended in dilute CH_3COOH, using the magnetic stand for collection after each wash. The fluorescence of the particles was measured using a fluorescence plate reader (Perkin-Elmer LS 5S, excitation wavelength 480 nm, slit width 10 nm, emission wavelength 510 nm, slit width 20 nm, emission cut-off 515 nm).

2.7. Cell capture using chitosan-mag

E. coli BL21 pGFP was cultured at 37 °C and 250 rpm in LB medium supplemented with ampicillin at 50 μg/mL. When the optical density OD_{600} of the cell culture was between 0.4 and 0.6, IPTG was added to induce GFP production (final concentration used was 1 mM IPTG). After 6 h induction, cells were collected by centrifugation at 6000g for 10 min at room temperature. The cells were resuspended in water with the pH adjusted using dilute CH_3COOH where needed. The pH was varied from 4 to 7.

For cell capture chitosan-mag in dilute CH_3COOH (0.5 mg/mL, pH varied from 4 to 7) was used. Capture was carried out at room temperature by using the cell suspension with the appropriate chitosan-mag suspension at the identical pH for 30 min. After capture, the particles were collected using the magnetic stand (specifications above) and washed thrice with double distilled water each time collecting the particles with the magnetic stand. After washing the particles were suspended in double distilled water at appropriate pH. The optical densities OD_{600} of the cell suspension before capture, of the supernatant after capture and of the three washes were measured. The optical density measurements were made simultaneously after the final wash and the amount of growth taking place during the capture and wash process was assumed to be minimal. To determine the amount of cells on the particles, the fluorescence of the resuspended particles with the attached cells was measured using a fluorescence plate reader mentioned above (excitation wavelength 395 nm, slit width 10 nm, emission wavelength 510 nm, slit width 10 nm, emission cut-off 430 nm). To determine the amount of cells captured in terms of difference in optical density, the following formula was used: $\Delta OD_{600} = OD_{cellsuspension} - OD_{supernatant} - OD_{washes}$ accounting appropriately for dilution.

2.8. Nanofactory assembly: attaching $(His)_6$-Pfs-$(Tyr)_5$ and $(His)_6$-LuxS-$(Tyr)_5$ to chitosan-mag

Chitosan-mag in dilute CH_3COOH (0.5 mg/mL, pH 6) was reacted with $(His)_6$-Pfs-$(Tyr)_5$ of varying concentrations (10–150 μg/mL) using activating enzyme, tyrosinase (100 U/mL). The reaction was carried out for 1 h at 37 °C. After reaction, the particles with the attached Pfs (now referred to as nanofactories) were collected using a magnetic stand (details above). The nanofactories were washed thrice with double distilled water to remove unbound Pfs and resuspended and stored until further use. Similarly, chitosan-mag in dilute CH_3COOH (0.5 mg/mL, pH 6) was reacted with $(His)_6$-LuxS-$(Tyr)_5$ of varying concentrations (10–150 μg/mL) using activating enzyme tyrosinase (100 U/mL) and treated as above to obtain nanofactories with bound LuxS.

2.9. In vitro synthesis of AI-2

The nanofactories containing Pfs and those containing LuxS were combined to obtain nanofactories with AI-2 synthesis ability. The in vitro synthesis of AI-2 was carried out by the addition of SAH (0.5 mM in 100 mM Tris-HCl buffer pH 7.8) to the nanofactories (1 mg/mL, 0.5 mg chitosan-mag with bound Pfs and 0.5 mg chitosan-mag with bound LuxS, pH 6). The reaction was carried out for 2 h at 37 °C. After the specified time the reaction was arrested using chloroform. The nanofactories were centrifuged at 12,000g for 5 min. The 'enzyme-free' supernatants (now containing in vitro AI-2) were collected and stored at −20 °C until further use.

2.10. AI-2 activity assay

The AI-2 activity assay was carried out as described elsewhere (Surette and Bassler, 1998). Briefly, 20 μl of AI-2 assay sample (collected during the above synthesis reaction) was mixed with 180 μl of BB170 suspension prepared by 5000-fold dilution of an overnight culture with AB medium. AB medium was used as negative control and a 4 h conditioned LB medium from E. coli W3110 grown at 250 rpm was used as a positive control. Bioluminescence obtained from experimental samples was normalized to the bioluminescence obtained for the negative control. All assays were repeated at least thrice with separately prepared samples to confirm the reproducibility of AI-2 activity.

2.11. Localized synthesis and delivery of AI-2 at cell surface using magnetic nanofactories

E. coli ZK126 pLW11 and E. coli LW7 pLW11 were pre-cultured overnight at 37 °C and 250 rpm in LB medium supplemented with ampicillin at 100 μg/mL. A total of 0.5 mL of these overnight pre-cultures was diluted in 49.5 mL LB medium supplemented with 60 μg/mL ampicillin. These cultures were grown at 30 °C at 250 rpm. The nanofactories were assembled as mentioned above. At 2-h intervals (from 0 to 8 h), samples from these cell cultures were withdrawn. For each 2-h sample, the cells were collected by centrifugation at 6000g for 10 min at room temperature. Cell suspensions were prepared in 10 mM phosphate buffer (PB, pH 6). Cell capture was carried out at room temperature using the magnetic nanofactories (1 mg/mL chitosan-mag, 0.5 mg chitosan-mag with bound Pfs, 0.5 mg of chitosan-mag with bound LuxS, pH 6) or just chitosan-mag (negative control, 1 mg/mL, pH 6). The nanofactories or chitosan-mag with captured cells were recovered by using a magnetic stand (specifications above). The nanofactories or chitosan-mag were washed thrice and resuspended in PB (pH 6). OD_{600} of the cell suspensions, supernatants and washes were measured as mentioned above to determine the amount of captured cells as mentioned above. In vitro AI-2 was synthesized at the surface of the cells captured by the nanofactories or chitosan-mag by adding 0.5 mM SAH (37 °C, 2 h synthesis). After synthesis, the nanofactories and chitosan-mag with attached cells were recovered using the magnetic stand. A Miller assay (Miller, 1972) was performed to determine the AI-2-dependent β-galactosidase expression for the cells captured by the nanofactories and chitosan-mag.

To study the effect of localized synthesis and delivery, in vitro AI-2 was synthesized at the surface of the cells (E. coli LW7 pLW11; 8 h time-point) captured by the magnetic nanofactories (1 mg/mL, 0.5 mg chitosan-mag with bound

Pfs, 0.5 mg of chitosan-mag with bound LuxS, pH 6) by adding 0.5 mM SAH (37 °C, 2 h synthesis) to the reaction mixture. After synthesis, the nanofactories were recovered using the magnetic stand and the AI-2-dependent Miller units of β-galactosidase expression of captured cells was determined. The β-galactosidase expression was compared with that obtained for cells captured by chitosan-mag (1 mg/mL) with 50 μg/mL each of unbound Pfs and LuxS and 0.5 mM SAH (37 °C, 2 h synthesis) added to the reaction mixture, cells captured by chitosan-mag (1 mg/mL) with 0.5 mM SAH (37 °C, 2 h synthesis) added to the reaction mixture, unattached (free) cells with 50 μg/mL each of unbound Pfs and LuxS and 0.5 mM SAH (37 °C, 2 h synthesis) added to the reaction mixture or unattached cells with 0.5 mM SAH (37 °C, 2 h synthesis) added to the reaction mixture.

2.12. Electron microscopy

Transmission electron microscopy (TEM) images of the chitosan-mag particles were taken using a Zeiss EM10 CA microscope at the University of Maryland Biological Ultrastructure Facility. For the scanning electron microscopy (SEM) images of the nanofactories attached to the target cells, the nanofactories were assembled as described above and the cell capture was carried out as mentioned above at the 8 h time-point. After cell capture, the nanofactories were recovered and the washed thrice to remove any uncaptured cells or traces of cell broth with double distilled water. The cells captured on the nanofactories were first fixed with 2% glutaraldehyde and then with 1% osmium tetroxide. The samples were then dehydrated with 100% ethanol and dried using critical point drying technique. The samples were then mounted and coated with gold (Au): palladium (Pd) alloy and viewed using a Hitachi S-4700 microscope. For TEM images of the nanofactories attached to the cells, after capture the particles with attached cells were fixed first in 2% glutaraldehyde, then in 1% osmium tetroxide and finally in 2% uranyl acetate. The fixed samples were dehydrated in 100% ethanol. The samples were progressively infiltrated with increasing amounts of Spurr's resin mixture in propylene oxide. Following this, the samples were embedded in fresh Spurr's resin and incubated at 70 °C. After curing at the 70 °C, the samples were sectioned using a diamond tip microtome and the sections were viewed using a Zeiss EM10 CA microscope.

2.13. Statistical analysis

To determine significant differences between different groups of data for a single experiment, a single-factor ANOVA test was performed. The data were tested to see if they fulfilled the homogeneity of variance assumption. For experiments that had more than two groups of data, multiple comparison tests were performed to determine which group/groups were significantly different (higher or lower) than other groups. *indicates that the group is significantly different from other groups (higher or lower, $p<0.01$).

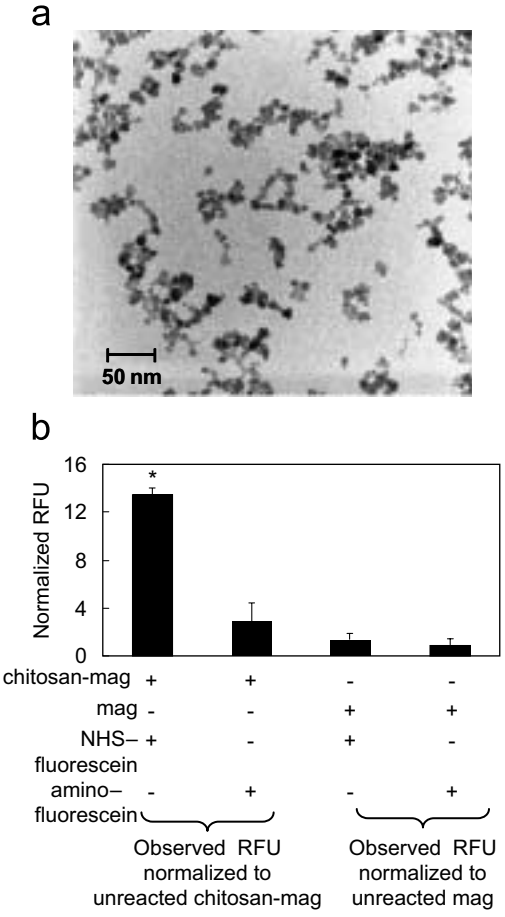

Fig. 2. Synthesis of the magnetic carrier chitosan-mag with accessible surface amine-groups of chitosan: (a) TEM of the synthesized chitosan-mag particles, (b) normalized relative fluorescence units (normalized RFU) produced by reacting chitosan-mag and mag with either NHS-fluorescein (amine-group reactive dye) or amino-fluorescein (control dye). *indicates significant difference ($p<0.01$).

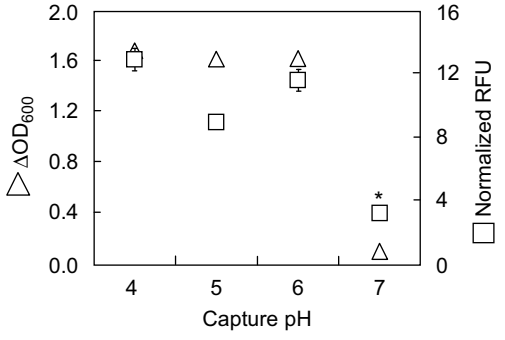

Fig. 3. Cell capture using chitosan-mag (cell capture ability). Optical density corresponding to the amount of cells captured by chitosan-mag as a function of pH (ΔOD_{600}, triangles) and measured normalized RFU of chitosan-mag with attached fluorescing cells (captured cells) as a function of pH (squares). *indicates significant difference ($p<0.01$).

3. Results

3.1. Synthesis of the magnetic carrier with accessible surface amine-groups of chitosan

The first step in the assembly of a magnetic nanofactory is the synthesis of the magnetic carrier 'chitosan-mag' (Fig. 1) by the dropwise addition of a mixture of ferrous and ferric chloride and chitosan into a vigorously stirred base (NH_4OH) under anoxic conditions (co-precipitation). Fig. 2a shows a transmission electron micrograph of the resultant chitosan-mag nanoparticles (average particle size ~10 nm). Surface accessibility of the amine-groups of chitosan (0.5 mg/mL, pH 6) is tested by labeling the nanoparticles with an amine-reactive fluorescent dye (5-(and 6)-carboxyfluorescein succinimidyl ester (NHS-fluorescein), 5 μg/mL, 30 min reaction at room temperature) (Fernandes et al., 2004). After reaction with NHS-fluorescein, the particles are collected using an external magnet and unreacted dye is removed by washing with double distilled water. Fig. 2b shows the Normalized relative fluorescence units (RFU) of NHS-fluorescein-labeled chitosan-mag particles compared to identically prepared controls (chitosan-mag particles reacted with

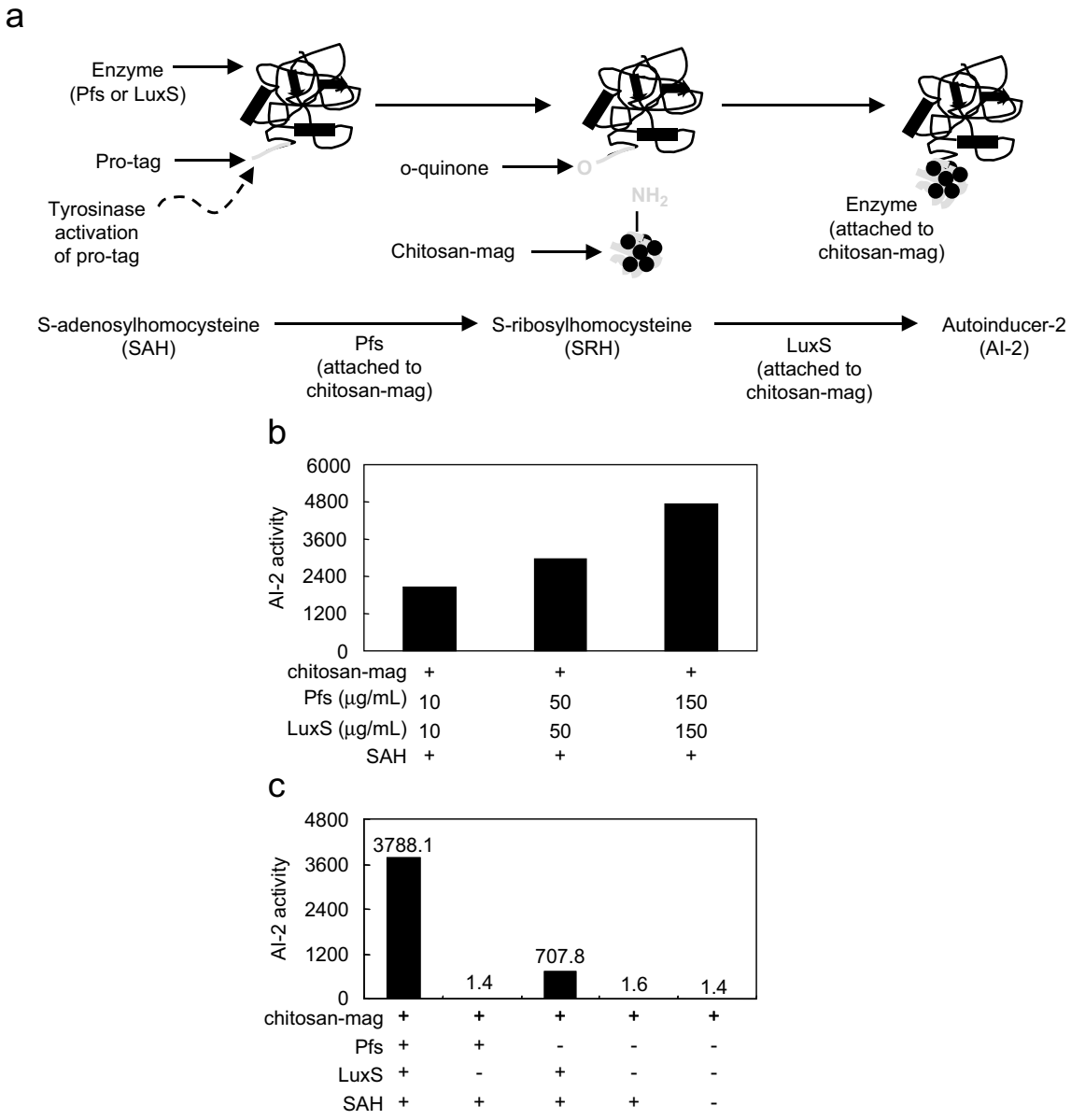

Fig. 4. Assembly of the magnetic nanofactories: attaching Pfs and LuxS to chitosan-mag via tyrosinase activatable pro-tags (synthesis ability): (a) attachment of the enzymes to chitosan-mag by activation of the pro-tags using tyrosinase; synthesis of AI-2 from substrate (SAH), the two-step synthesis is catalyzed by the enzymes Pfs and LuxS, (b) AI-2 activity observed in reporter strain in response to in vitro AI-2 synthesized by adding SAH to nanofactories containing varying (increasing) amounts of added Pfs and LuxS, (c) AI-2 activity observed in reporter strain in response to in vitro AI-2 synthesized by adding SAH to either the nanofactories or one or more element of the nanofactory.

((4′-aminoacetamido) methyl) fluorescein (amino-fluorescein) which is not directly amine-reactive, NHS-fluorescein-labeled magnetite (mag) nanoparticles without chitosan and mag particles reacted with amino-fluorescein). The fluorescence of chitosan-mag labeled with NHS-fluorescein is ~13.5-fold higher than that of chitosan-mag without NHS-fluorescein, ~4.5-fold higher than chitosan-mag reacted with amino-fluorescein, ~9.5-fold higher than mag with NHS-fluorescein and ~15.5-fold higher than mag with amino-fluorescein. These results confirm that amine-reactive NHS-fluorescein preferentially binds to chitosan and that chitosan-mag particles have abundant amine-reactive sites.

3.2. Cell capture using chitosan-mag (cell capture ability)

Chitosan-mag particles (0.5 mg/mL) are tested for their ability to capture cells via accessible surface chitosan (cell capture ability) by adding the particles to a suspension containing fluorescing cells [E. coli BL21 pGFP induced with 1 mM IPTG to produce green fluorescent protein (GFP) (Wu et al., 2000)]. The particles are contacted with the fluorescing cells for 30 min at room temperature. Because chitosan's amines confer pH-sensitive net charge, we investigated the effect of pH on cell capture over a range of pH (from pH 4 to 7). After capture, the particles with the attached cells are recovered with an external magnet and rinsed 3 times with double distilled water to remove the unbound cells. The optical density at 600 nm (OD_{600}) of the cell suspension before capture, the supernatant after capture and the washes are measured to estimate the amount of captured cells. The difference in optical density, ΔOD_{600}, ($\Delta OD_{600} = OD_{cellsuspension} - OD_{supernatant} - OD_{washes}$ accounting appropriately for the dilutions) corresponds to the optical density of the captured cells. The fluorescence of the resuspended particles with the attached cells is also measured using a fluorescence plate reader as a second way of estimating the amount captured cells. Fig. 3 shows ΔOD_{600} (the optical density of the captured cells) and the measured normalized RFU of the particles plus attached cells (fluorescence of chitosan-mag with captured cells divided by that of chitosan-mag without cells) as a function of pH. The cell capture by chitosan-mag is observed to be higher at lower pH ($\leqslant 6$) and decreases as the pH is increased to 7. The capture was found to remain low when the pH was increased above 7 (data not shown) (Honda et al., 1998). This indicates that chitosan-mag can be used for cell capture ($pH \leqslant 6$). We use pH 6 for subsequent experiments involving cell capture.

3.3. Assembly of magnetic nanofactories: attaching Pfs and LuxS to chitosan-mag via tyrosinase activatable pro-tags (synthesis ability)

The QS enzymes, Pfs and LuxS, are both engineered to have hexahistidine-tags at their N-termini and pro-tags (pentatyrosine-tags) at their C-termini [viz. $(His)_6$-Pfs-$(Tyr)_5$ and $(His)_6$-LuxS-$(Tyr)_5$]. The hexahistidine tags at the N-termini are used to obtain the purified enzymes via immobilized metal ion affinity chromatography (IMAC). The pro-tags at the C-termini are used to increase the amount of accessible tyrosine residues for the reaction conjugating the enzymes to chitosan. They facilitate formation of the enzyme-chitosan conjugate with intact enzymatic activity. Tyrosinase is used to activate the pro-tag; it converts accessible tyrosine residues to reactive o-quinones (Chen et al., 2001, 2002, 2003). These electrophilic o-quinones can then react non-enzymatically with the nucleophilic amine-groups of accessible surface chitosan to form Schiff bases or Michael-type adducts that couple the enzymes on to chitosan (Lewandowski et al., 2006) (Fig. 4a and Fig. S1).

In our experiments, we first attach Pfs to chitosan-mag (0.5 mg/mL, pH 6) by activation of its pro-tag using tyrosinase (100 U/mL). The concentration of added Pfs is varied [10 μg/mL (0.34 μM), 50 μg/mL (1.70 μM) or 150 μg/mL (5.10 μM)]. After reaction, the nanofactories with Pfs are recovered by an external magnet and rinsed thrice with distilled water to remove any unbound enzyme. Similarly, we assemble magnetic nanofactories with LuxS by attaching LuxS to chitosan-mag (0.5 mg/mL, pH 6) using tyrosinase (100 U/mL) and varying concentrations of added LuxS [concentrations 10 μg/mL (0.40 μM), 50 μg/mL (2.00 μM) or 150 μg/mL (6.00 μM)]. Studies calculating the amount of pro-tagged proteins bound to chitosan (i.e. mg of bound protein/mg of chitosan) upon tyrosinase activation can be found elsewhere (Lewandowski et al., 2006). The nanofactories with Pfs and those with LuxS are then combined to form a single solution with AI-2 synthesis ability (containing both types of magnetic nanofactories). The nanofactories synthesize in vitro AI-2 upon addition of the substrate SAH (Fig. 4a; 0.5 mM, 37 °C, 2 h reaction). The reaction is arrested and the reaction mixture is analyzed to determine the amount of in vitro AI-2. Here, 'enzyme-free' solutions containing AI-2 are added to a suspension containing a reporter bacterial strain Vibrio harveyi BB170 (Bassler et al., 1993) which produces light in response to added AI-2 (Surette and Bassler, 1998). The luminescence produced indicates the AI-2 activity in the added sample. Fig. 4b shows the AI-2 activity (luminescence produced by V. harveyi with AI-2 in added sample divided by that produced without AI-2 in added sample) for varying amounts of added enzymes (Pfs and LuxS, 10–150 μg/mL). The AI-2 activity increases with increasing amounts of added enzymes.

For in vitro AI-2 synthesis ability, we expect that both types of nanofactory (i.e. with attached Pfs and LuxS) and substrate SAH need to be present. To test this, in vitro AI-2 synthesis was carried out using combinations of the above elements (when used: 1 mg/mL chitosan-mag, 0.5 mM SAH, 50 μg/mL Pfs and 50 μg/mL LuxS). Fig. 4c shows that the observed AI-2 activity is much higher when all elements for AI-2 synthesis are simultaneously present,

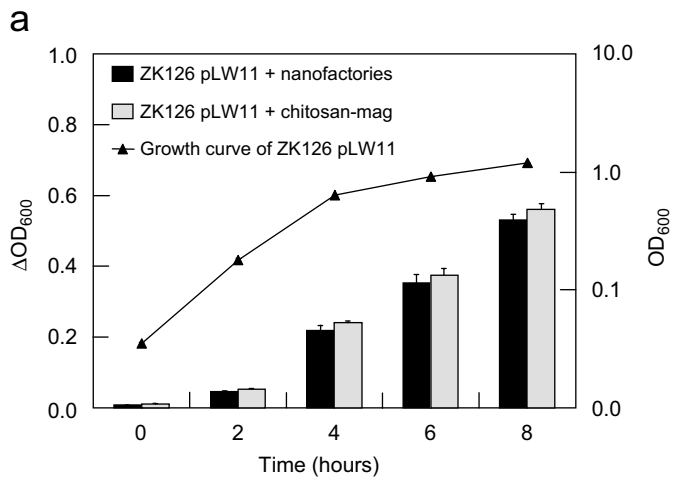
a
ZK126 pLW11 + nanofactories
ZK126 pLW11 + chitosan-mag
Growth curve of ZK126 pLW11
ΔOD600
OD600
Time (hours)

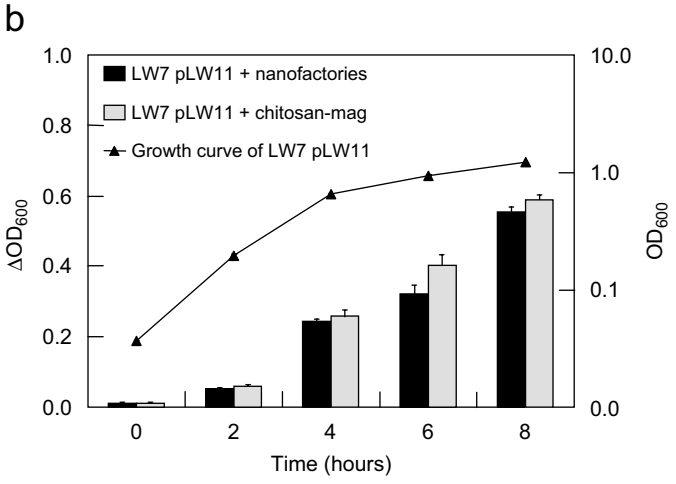
b
LW7 pLW11 + nanofactories
LW7 pLW11 + chitosan-mag
Growth curve of LW7 pLW11
ΔOD600
OD600
Time (hours)

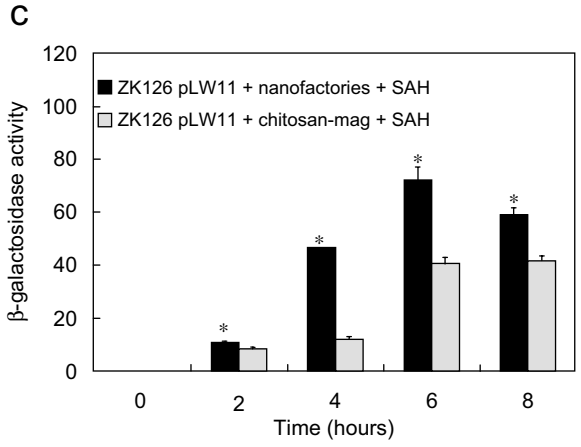
c
ZK126 pLW11 + nanofactories + SAH
ZK126 pLW11 + chitosan-mag + SAH
β-galactosidase activity
Time (hours)

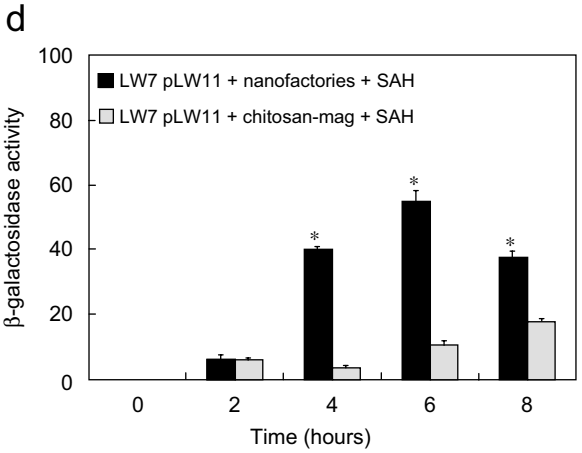
d
LW7 pLW11 + nanofactories + SAH
LW7 pLW11 + chitosan-mag + SAH
β-galactosidase activity
Time (hours)


e


f
1 μm

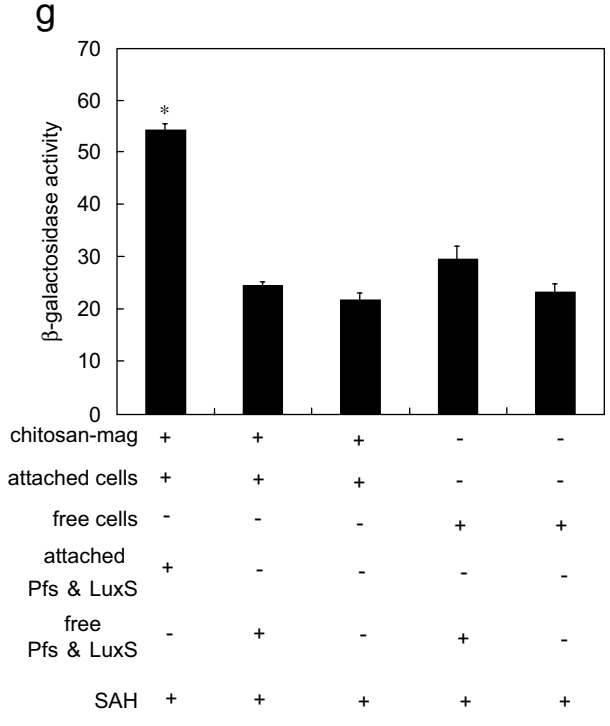
g
β-galactosidase activity
chitosan-mag + + + - -
attached cells + + + - -
free cells - - - + +
attached Pfs & LuxS + - - - -
free Pfs & LuxS - + - + -
SAH + + + + +

~4-fold lower in the case of nanofactories with only attached LuxS and added SAH, and negligible for all other cases.

3.4. Localized synthesis and delivery of in vitro AI-2 at the cell surface using magnetic nanofactories

To demonstrate user-specified localized synthesis and delivery of AI-2, cultures of E. coli are grown in shake flask cultures, exposed to magnetic nanofactories, and evaluated for phenotypic response in a set of controlled experiments. The magnetic nanofactories are assembled (1 mg/mL chitosan-mag; 0.5 mg chitosan-mag with 50 μg/mL Pfs and 0.5 mg chitosan-mag with 50 μg/mL LuxS) and added to a growing suspension of either E. coli ZK126 pLW11 (Connell et al., 1987) or E. coli LW7 pLW11 (pH 6) for cell capture (Wang et al., 2005). E. coli ZK126 is a lac null mutant while E. coli LW7 is a lac and luxS double mutant. The plasmid, pLW11, employs the lsr promoter (AI-2 responsive) to drive β-galactosidase expression (Wang et al., 2005).

Cell capture is performed at 2-h intervals throughout the experiments (from inoculation to stationary phase). There is no apparent difference in capture efficiency due to the added enzymes in the case of the nanofactories (Fig. 5a and b). After capture, the nanofactories with the attached cells are recovered using an external magnet and unbound cells are rinsed off (phosphate buffer, PB).

After capture, in vitro AI-2 is synthesized by the nanofactories at the cell surface by the addition of SAH (0.5 mM, 37 °C, 2 h reaction). Functioning nanofactories are demonstrated by AI-2 synthesis and delivery at the surface of these cells, followed by AI-2 transport and altered gene expression (as determined by AI-2-dependent β-galactosidase expression). In Fig. 5c and d, AI-2-dependent β-galactosidase expression is compared to the negative controls (Fig. 5c for E. coli ZK126 pLW11 and Fig. 5d for E. coli LW7 pLW11). In the case of $LuxS^+$ cells (ZK126), which synthesize their own AI-2, the increase in β-galactosidase expression is enhanced ~4-fold due to the AI-2 synthesized at the cell surface. In the case of $luxS^-$ cells (LW7), the increase is >10-fold. These results clearly indicate altered phenotypic behavior and a functioning 'programmable' nanofactory. Fig. 5e and f show SEM and TEM images of the nanofactories attached to E. coli LW7 pLW11.

To study the benefit of localized synthesis and delivery of AI-2, the nanofactories are compared to various other configurations using either free cells or cells attached to chitosan-mag (1 mg/mL) either with or without the addition of free enzymes (Pfs and LuxS 50 μg/mL). The control experiments are designed to synthesize equivalent levels of AI-2. In Fig. 5g, the cell response to AI-2 delivered locally via nanofactories is 2-fold higher than that observed for delivery by diffusion from the bulk. Our cell surface approach using the magnetic nanofactories produces the highest AI-2-dependent β-galactosidase expression indicating that localized synthesis and delivery of AI-2 results in an increased AI-2-specific transcriptional response.

4. Discussion

We have demonstrated magnetic nanofactories for the localized synthesis and delivery of the QS signaling molecule AI-2 to the surface of E. coli. Our magnetic nanofactories consist of E. coli AI-2 synthases, Pfs and LuxS, attached to nano-sized co-precipitates of chitosan-mag (Fig. 2a). They possess the ability to manufacture AI-2 (via attached Pfs and LuxS; synthesis ability), to attach to the cell surface (via chitosan; cell capture ability) and to be directed and recovered in response to an external magnetic field (via magnetite; stimuli responsiveness).

The biopolymer chitosan serves a dual role in the nanofactory viz. enabling cell capture and providing amine groups to attach Pfs and LuxS. This dual role is attributed to chitosan's unique pH-dependent behavior, particularly the reversible protonation–deprotonation of the amine-groups of chitosan. The decrease in the cell capture ability of chitosan-mag as the pH is increased above 6 (Fig. 3) is due to the increased extent of amine deprotonation at pH values above their pK_a (no net charge). For attaching QS enzymes, chitosan's amine-groups should be in nucleophilic (neutral) form. We selected a pH of 6 for our work because at this pH there are sufficient deprotonated amines for enzyme assembly while retaining protonated amines needed for capture (Fig. 5a and b). Incidentally, as noted by capture efficiency experiments (Fig. 5a and b) and enzyme loading experiments (Fig. 4b) we have not exhausted the available amines from chitosan for either capture or enzyme loading. This may be advantageous should one need to assemble a cell-specific targeting moiety to the nanofactories.

Fig. 5. Localized synthesis and delivery of in vitro AI-2 at the target cell surface using magnetic nanofactories. (a) $LuxS^+$: Cell capture using magnetic nanofactories: Δ optical density of cells captured by the nanofactories at various time-points for E. coli ZK126 pLW11 (ΔOD_{600}; columns) and corresponding growth curve. (b) $LuxS^-$: Cell capture using magnetic nanofactories: Δ optical density of cells captured by the nanofactories at various time-points for E. coli LW7 pLW11 (ΔOD_{600}; columns) and corresponding growth curve. (c) $LuxS^+$: AI-2-dependent β-galactosidase activity produced in response to synthesis and delivery of AI-2 by nanofactories to the surface of the target cells (E. coli ZK126 pLW11, Miller units). *indicates significant difference ($p<0.01$). (d) $LuxS^-$: AI-2-dependent β-galactosidase activity produced in response to synthesis and delivery of AI-2 by nanofactories to the surface of the target cells (E. coli LW7 pLW11, Miller units). *indicates significant difference ($p<0.01$). (e) SEM of the nanofactories attached to the target cells, E. coli LW7 pLW11. (f) TEM of nanofactories attached to the target cells, E. coli LW7 pLW11. (g) AI-2-dependent β-galactosidase activity produced in response to localized synthesis and delivery of AI-2 by nanofactories to the surface of the target cells (E. coli LW7 pLW11) compared to that produced using other techniques of AI-2 synthesis and delivery. *indicates significant difference ($p<0.01$).

The enzymes Pfs and LuxS contain activatable pro-tags at their C-termini. The pro-tag extends away from the active site of both enzymes and also provides tyrosine residues for the activation by tyrosinase hence facilitating the attachment of the enzymes to chitosan-mag with intact activity (due to the mild reaction conditions; Fig. 4b). This report is the first demonstration of small molecule synthesis using enzymes with engineered pro-tags.

The nanofactories with synthesis ability, cell capture ability and stimuli responsiveness are used to capture the strains E. coli ZK126 pLW11 (Fig. 5a) and E. coli LW7 pLW11 (Fig. 5b, e and f). The synthesis and delivery of AI-2 at the surface of the captured cells using the nanofactories results in increased AI-2-dependent β-galactosidase expression for both strains (Fig. 5c and d). The use of nanofactories for the localized synthesis and delivery of AI-2 also produces an increase in AI-2-dependent β-galactosidase expression when compared to other techniques of synthesis and delivery of AI-2 (Fig. 5g indicating the benefit of localized synthesis and delivery in producing increased AI-2-specific transcriptional response (β-galactosidase reporter expression).

We believe our work is significant for the following reasons. Our technique of using magnetic nanofactories to locally synthesize and deliver signaling molecules to target cell surfaces is novel. The magnetic nanofactories have diverse, yet co-existent attributes of small molecule synthesis ability, cell capture ability and responsiveness to external magnetic fields, which make them suitable for use in localized cell surface synthesis and delivery applications. The cell capture ability of the nanofactories is based on the simple, reversible pH-dependent properties of chitosan. While this charge based capture of cells by chitosan is non-specific, specificity can be bestowed to the nanofactory by using an appropriate antibody to a particular region of the target cell. Standard amine-group chemistry of chitosan can be used to attach the antibody to the nanofactory. Further investigations on this aspect are currently in progress. An external (non-invasive) magnetic field is used to recover the nanofactories with attached cells and confine them to a specific location for further analysis. The increase in AI-2-specific transcriptional response (β-galactosidase reporter expression) particularly at earlier times (4- and 6-h time-points) for both strains indicates functioning and programmable nanofactories that are successful in intercepting and modulating cell–cell communication. Thus, we have a facile tool to modulate QS with a view to understanding and controlling QS-based phenomena such as biofilm formation, pathogenicity, and antibiotic resistance. Finally, we believe nanofactories offer many advantages relative to the localized delivery of small molecules, in that the molecule could eventually be synthesized and delivered at a site, at a prescribed concentration and time.

Acknowledgments

Partial support of this work was provided by the National Science Foundation (Grant No. BES-0124401) and the Bioengineering Graduate Program of the University of Maryland (fellowship to RF).

Appendix A. Supplementary data

Supplementary data associated with this article can be found in the online version at doi:10.1016/j.ymben.2006.11.004.

References

Bassler, B.L., Wright, M., Showalter, R.E., Silverman, M.R., 1993. Intercellular signalling in Vibrio harveyi: sequence and function of genes regulating expression of luminescence. Mol. Microbiol. 9, 773–786.

Bassler, B.L., Wright, M., Silverman, M.R., 1994. Multiple signalling systems controlling expression of luminescence in Vibrio harveyi: sequence and function of genes encoding a second sensory pathway. Mol. Microbiol. 13, 273–286.

Cadieux, N., Bradbeer, C., Reeger-Schneider, E., Koster, W., Mohanty, A.K., Wiener, M.C., Kadner, R.J., 2002. Identification of the periplasmic cobalamin-binding protein BtuF of E. coli. J. Bacteriol. 184, 706–717.

Chen, T.H., Vazquez-Duhalt, R., Wu, C.F., Bentley, W.E., Payne, G.F., 2001. Combinatorial screening for enzyme-mediated coupling. Tyrosinase-catalyzed coupling to create protein–chitosan conjugates. Biomacromolecules 2, 456–462.

Chen, T.H., Embree, H.D., Wu, L.Q., Payne, G.F., 2002. In vitro protein–polysaccharide conjugation: tyrosinase-catalyzed conjugation of gelatin and chitosan. Biopolymers 64, 292–302.

Chen, T.H., Small, D.A., Wu, L.Q., Rubloff, G.W., Ghodssi, R., Vazquez-Duhalt, R., Bentley, W.E., Payne, G.F., 2003. Nature-inspired creation of protein–polysaccharide conjugate and its subsequent assembly onto a patterned surface. Langmuir 19, 9382–9386.

Chung, Y.I., Tae, G., Hong Yuk, S., 2006. A facile method to prepare heparin-functionalized nanoparticles for controlled release of growth factors. Biomaterials 27, 2621–2626.

Connell, N., Han, Z., Moreno, F., Kolter, R., 1987. An E. coli promoter induced by the cessation of growth. Mol. Microbiol. 1, 195–201.

Fernandes, R., Wu, L.Q., Chen, T.H., Yi, H.M., Rubloff, G.W., Ghodssi, R., Bentley, W.E., Payne, G.F., 2003. Electrochemically induced deposition of a polysaccharide hydrogel onto a patterned surface. Langmuir 19, 4058–4062.

Fernandes, R., Yi, H.M., Wu, L.Q., Rubloff, G.W., Ghodssi, R., Bentley, W.E., Payne, G.F., 2004. Thermo-biolithography: a technique for patterning nucleic acids and proteins. Langmuir 20, 906–913.

Fuqua, W.C., Winans, S.C., Greenberg, E.P., 1994. Quorum sensing in bacteria: the LuxR-LuxI family of cell density-responsive transcriptional regulators. J. Bacteriol. 176, 269–275.

Geer, D.J., Swartz, D.D., Andreadis, S.T., 2005. Biomimetic delivery of keratinocyte growth factor upon cellular demand for accelerated wound healing in vitro and in vivo. Am. J. Pathol. 167, 1575–1586.

Gonzalez Barrios, A.F., Zuo, R., Hashimoto, Y., Yang, L., Bentley, W.E., Wood, T.K., 2006. Autoinducer 2 controls biofilm formation in E. coli through a novel motility quorum-sensing regulator (MqsR, B3022). J. Bacteriol. 188, 305–316.

Henke, J.M., Bassler, B.L., 2004. Bacterial social engagements. Trends Cell. Biol. 14, 648–656.

Holland, T.A., Bodde, E.W., Cuijpers, V.M., Baggett, L.S., Tabata, Y., Mikos, A.G., Jansen, J.A., 2006. Degradable hydrogel scaffolds for in vivo delivery of single and dual growth factors in cartilage repair. Osteoarthritis Cartilage.

Honda, H., Kawabe, A., Shinkai, A., Kobayashi, T., 1998. Development of chitosan-conjugated magnetite for magnetic cell separation. J. Ferment. Bioeng. 86, 191–196.

Honda, H., Kawabe, A., Skinkai, M., Kobayashi, T., 1999. Recovery of recombinant E. coli by chitosan-conjugated magnetite. Biochem. Eng. J. 3, 157–160.

Koop, A.H., Hartley, M.E., Bourgeois, S., 1987. A low-copy-number vector utilizing beta-galactosidase for the analysis of gene control elements. Gene 52, 245–256.

Lee, J.P., Jalili, R.B., Tredget, E.E., Demare, J.R., Ghahary, A., 2005. Antifibrogenic effects of liposome-encapsulated IFN-alpha2b cream on skin wounds in a fibrotic rabbit ear model. J. Interferon Cytokine Res. 25, 627–631.

Lewandowski, A., Small, D., Chen, T., Payne, G., Bentley, W., 2006. Tyrosine based "activatable pro-tag" enzyme catalyzed protein capture and release. Biotechnol. Bioeng. 93, 1207–1215.

Miller, J., 1972. Experiments in Molecular Genetics. Cold Spring Harbor Laboratory Press, Cold Spring Harbor.

Shansky, J., Creswick, B., Lee, P., Wang, X., Vandenburgh, H., 2006. Paracrine release of insulin-like growth factor 1 from a bioengineered tissue stimulates skeletal muscle growth in vitro. Tissue Eng. 12, 1833–1841.

Shiner, E.K., Rumbaugh, K.P., Williams, S.C., 2005. Inter-kingdom signaling: deciphering the language of acyl homoserine lactones. FEMS Microbiol. Rev. 29, 935–947.

Surette, M.G., Bassler, B.L., 1998. Quorum sensing in E. coli and Salmonella typhimurium. Proc. Natl. Acad. Sci. USA 95, 7046–7050.

Taylor, L., Jones, L., Tuszynski, M.H., Blesch, A., 2006. Neurotrophin-3 gradients established by lentiviral gene delivery promote short-distance axonal bridging beyond cellular grafts in the injured spinal cord. J. Neurosci. 26, 9713–9721.

Truckses, D.M., Bloomekatz, J.E., Thorner, J., 2006. The RA domain of Ste50 adaptor protein is required for delivery of Ste11 to the plasma membrane in the filamentous growth signaling pathway of the yeast Saccharomyces cerevisiae. Mol. Cell Biol. 26, 912–928.

Vendeville, A., Winzer, K., Heurlier, K., Tang, C.M., Hardie, K.R., 2005. Making 'sense' of metabolism: autoinducer-2, LuxS and pathogenic bacteria. Nat. Rev. Microbiol. 3, 383–396.

Wang, L., Hashimoto, Y., Tsao, C.Y., Valdes, J.J., Bentley, W.E., 2005. Cyclic AMP (cAMP) and cAMP receptor protein influence both synthesis and uptake of extracellular autoinducer 2 in E. coli. J. Bacteriol. 187, 2066–2076.

Wang, B., Li, S., Southern, P.J., Cleary, P.P., 2006. Streptococcal modulation of cellular invasion via TGF-beta1 signaling. Proc. Natl. Acad. Sci. USA 103, 2380–2385.

Waters, C.M., Bassler, B.L., 2005. Quorum sensing: cell-to-cell communication in bacteria. Annu. Rev. Cell Dev. Biol. 21, 319–346.

Wei, G., Jin, Q., Giannobile, W.V., Ma, P.X., 2006. Nano-fibrous scaffold for controlled delivery of recombinant human PDGF-BB. J. Control Release 112, 103–110.

Winzer, K., Hardie, K.R., Williams, P., 2002. Bacterial cell-to-cell communication: sorry, can't talk now—gone to lunch!. Curr. Opin. Microbiol. 5, 216–222.

Wu, C.F., Cha, H.J., Rao, G., Valdes, J.J., Bentley, W.E., 2000. A green fluorescent protein fusion strategy for monitoring the expression, cellular location, and separation of biologically active organophosphorus hydrolase. Appl. Microbiol. Biotechnol. 54, 78–83.

Wu, L.Q., Gadre, A.P., Yi, H.M., Kastantin, M.J., Rubloff, G.W., Bentley, W.E., Payne, G.F., Ghodssi, R., 2002. Voltage-dependent assembly of the polysaccharide chitosan onto an electrode surface. Langmuir 18, 8620–8625.

Xavier, K.B., Bassler, B.L., 2005. Interference with AI-2-mediated bacterial cell–cell communication. Nature 437, 750–753.

Yang, S., Lopez, C.R., Zechiedrich, E.L., 2006. Quorum sensing and multidrug transporters in E. coli. Proc. Natl. Acad. Sci. USA.